R-3/D2 #59

Enclosure IV to
ML-95-014

COMBUSTION ENGINEERING, INC.

MODEL UNC-2901 FUEL PELLET/POWDER SHIPPING CONTAINER

CERTIFICATE OF COMPLIANCE NO. 6294

APPLICATION CHANGE PAGES

April 1995

II-16

TABLE OF CONTENTS

UNC-2901 Shipping Container

1. GENERAL INFORMATION

1.1 Introduction

The UNC-2901 container is designed for shipment of uranium oxide pellets manufactured, inspected and certified in accordance with reactor fuel specifications. It can also be used for the shipment of dry uranium compounds such as uranium oxide powder and rejected pellets and pieces (hard scrap).

The maximum number of containers per shipment shall be limited to:

Fissile Class I	-	None
Fissile Class II	-	(Maximum 100 containers; Transport index is 0.50 per container, for a total transport index of 50 per shipment).
Fissile Class III	-	Maximum 100 containers

1.2 Package Description

1.2.1 Packaging

The UNC-2901 container consists of a standard steel drum (see Drawing D-5007-8086, Rev. 6) with a 10 3/4" square inner container centered in the drum. The inner container is centered by hardboard support rings. Asbestos or ceramic sheet, plywood and Fiberlite insulation provide thermal protection to the inner container. The inner container closure is fitted with a gasket capable of withstanding temperatures up to at least 500°F. The UNC-2901 containers are shipped either two (2) or three (3) to a shipping pallet in horizontal or vertical orientations, respectively. Only the inner container internal support package assembly differs between shipping package configurations.

1.2.1.1 Package for Pellets

In the horizontal shipping orientation, the uranium oxide pellet package consists of either of two options: covered bulk pellet pans which can be stacked to a maximum of 16 pans (4 high x 2 wide x 2 deep), or corrugated trays which can be stacked to a maximum of 42 pellet trays (plus one cover tray).

For the bulk pellet pans, each row of pans is secured with a single piece weblock strapping assembly. The weblock buckle is part of the tray holder and the buckle is attached to the holder by a rod and angle bracket assembly. A typical arrangement is depicted in Drawing D-5018-2001, Rev. 01.

For the corrugated pellet trays, the trays are similarly secured to the tray holder with weblock strapping. Wood spacer blocks are used to minimize void space; the loaded tray holder is contained within a stainless steel shell. The arangement is depicted in Drawing D-5018-2011, Revision 0.

Herein, the term "bulk pellet tray" (as opposed to "corrugated tray") should be understood to mean, for most purposes, the same as "bulk pellet pan".

In the vertical shipping orientation the uranium oxide pellet package consists of covered bulk pellet pans which can be stacked to a maximum of 16 pans (8 high x 2 wide). The stack of pans is held in place by a vise type arrangement which is part of the vertical shipping cradle assembly inserted into the inner container. A typical arrangement is depicted in Drawing NFM-E-4661, Rev. 02.

1.2.1.2 Package for Dry Compounds

Uranium oxide powder is packaged in a plastic bag within a stainless steel UO_2 powder can (specified on Drawing NPM-C-3389). A maximum of two UO_2 powder cans are packaged in a UNC-2901 shipping container in accordance with the requirements of Drawing NFM-D-4752, Rev. 01. Shipment of UO_2 powder is done using the same inner container insert assembly independent of horizontal or vertical shipping orientations.

1.2.1.3 Package for Reject Powder/Pellets

Rejected uranium oxide pellets and pieces may be packaged in any of the pellet shipping package configurations described above, with the exception of corrugated trays (see Section 1.2.1.1). Likewise, rejected uranium oxide powder may be packaged as described in Section 1.2.1.2 for virgin powder.

1.2.2 Operational Features

The UNC-2901 shipping container is of relatively simple design, and does not incorporate cooling systems, shielding, etc.

1.2.3 Contents of Packaging

Pellets or reject pellets are shipped in bulk pellet pans in either the horizontal or vertical shipping orientation. Pellets are also shipped in corrugated trays in the horizontal configuration; corrugated trays are not used to ship reject pellets or pieces. UO_2 powder is shipped in powder cans in either the horizontal or verticle shipping configuration.

1.2.3.1 Pellets or Rejected Pellets - in Bulk Pellet Pans

Maximum Enrichment: 5.0 wt.%

Type Material: Sintered (high fired) uranium oxide pellets, rejected pellets or pieces.

Maximum quantity per container:

a) Maximum net weight of pellets: 320 pounds
Maximum net weight of pellets and packaging material (contents of inner container): 427 pounds.

b) Gross weight of the container as assembled for shipment shall not exceed 660 pounds.

1.2.3.2 Pellets - in Corrugated Trays

Maximum Enrichment: 5.0 wt.%

Type Material: Sintered (high fired) uranium oxide pellets.

Maximum quantity per container:

a) Maximum net weight of pellets: 136.5 Kg

b) Gross weight of the container as assembled for shipment shall not exceed 660 pounds.

1.2.3.3 Dry Compounds or Rejected Powder

Maximum Enrichment: 5.0 wt.%

Type Material: Uranium Oxide powder or rejected powder.

Maximum quantity per container:

a) Maximum net weight (powder or rejected powder): 77.2 pounds (35.0 Kg) at maximum enrichment.

The analytic expression for the maximum Kg UO_2 per package is simply (175.0/(w/o U-235)) Kg $_{UO2}$. This expression is based on limiting the total U-235 to that computed at 5 w/o.

b) Gross weight of container as assembled for shipment shall not exceed 457 pounds.

1.3 Appendix

Details of construction and assembly are shown on drawings:

Drawing No.	Revision	Title
D-5007-8086	6	S.W.O.P.P. Upgrade UNC 2901 Shipping Drum for UO_2 Powder & Pellets Assembly & Details
B-5007-8112	1	Suggested Assembly of 2901 Plywood Insert
D-5018-2001	1	Pellet Shipping Package, 16 Trays (Pellets) in 2901
NFM-D-4263	2	Pellet Tray Holder
NPM-C-3389	0	UO_2 Inner Container
NPM-C-3389	3	UO_2 Inner Container
NFM-E-4661	2	Bulk Pellet Shipping Tray Assembly
NFM-D-4721	1	Pellet Tray Cover Assembly
NFM-D-4540	1	Cage Assembly 2901 Shipping Drum
D-5018-2011	0	UNC-2901 Shipping Arangement Using Corrugated Trays
AA-257-457	0	ABB Atom, Transport Och Forvar Ings - Bricka For Kutsar (Corrugated Tray)
C-5018-2012	0	Pellet Tray Packaged Bundle
C-5018-2013	0	Wood Spacers for Corrugated Tray Shipments

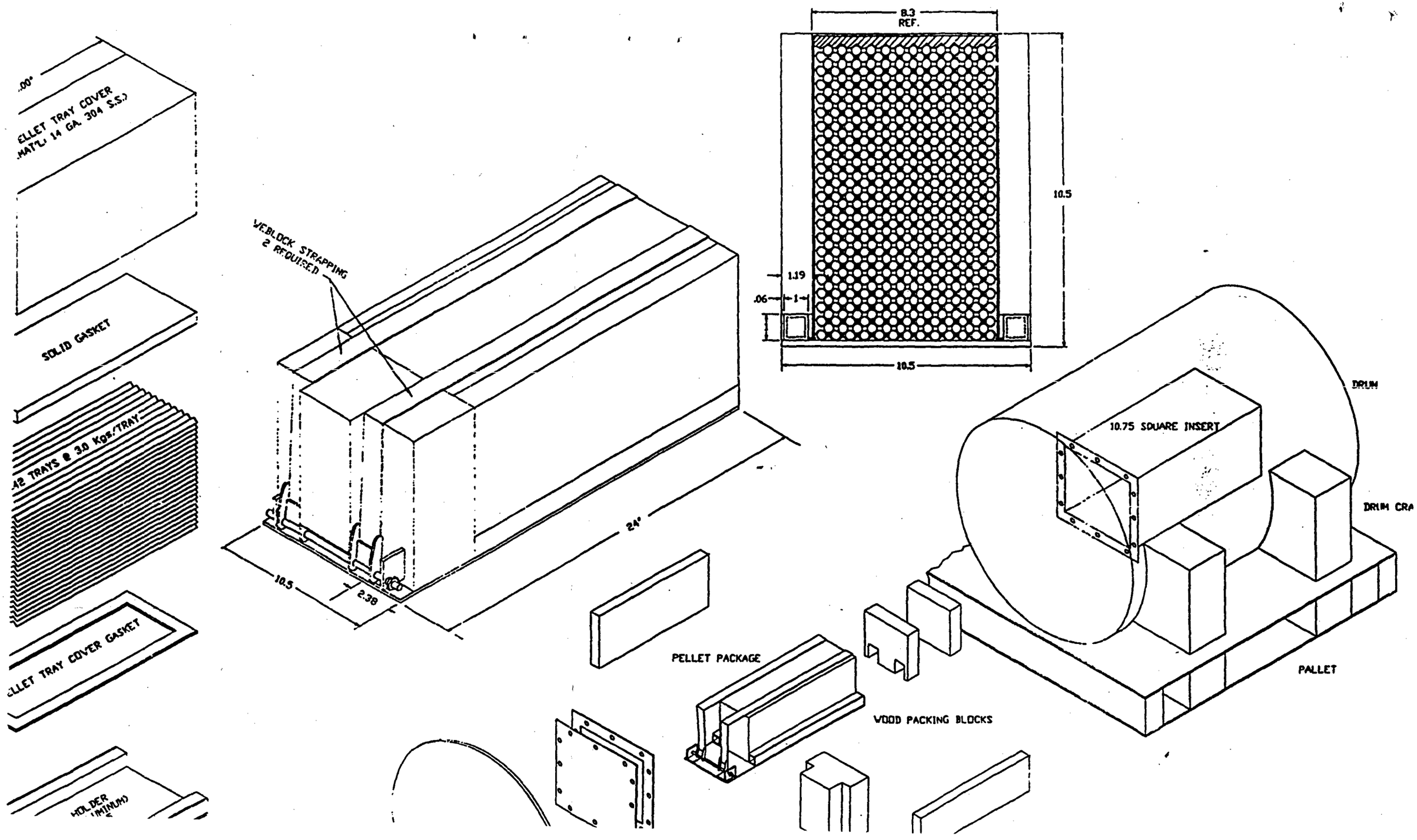
.00"
ELLET TRAY COVER
MAT'L: 14 GA. 304 S.S.)
SOLID GASKET
42 TRAYS @ 3.0 Kgs/TRAY
ELLET TRAY COVER GASKET
HOLDER
WEBLOCK STRAPPING
2 REQUIRED
24"
10.5
2.38
8.3
REF.
10.5
1.19
.06
1
10.5
DRUM
10.75 SQUARE INSERT
DRUM CRA
PALLET
PELLET PACKAGE
WOOD PACKING BLOCKS

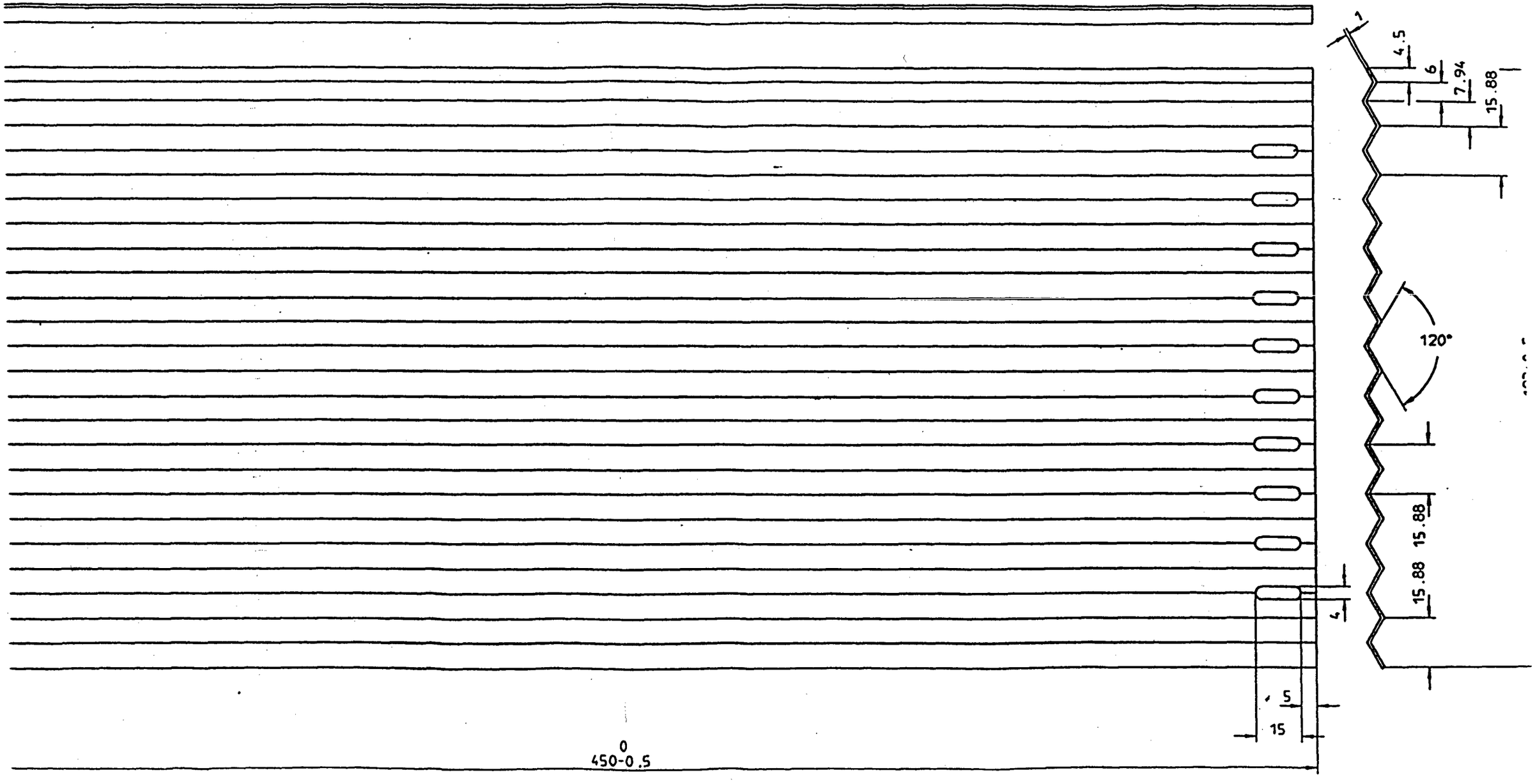
1
4.5
6
7.94
15.88
120°
15.88
15.88
4
5
15
0
450-0.5

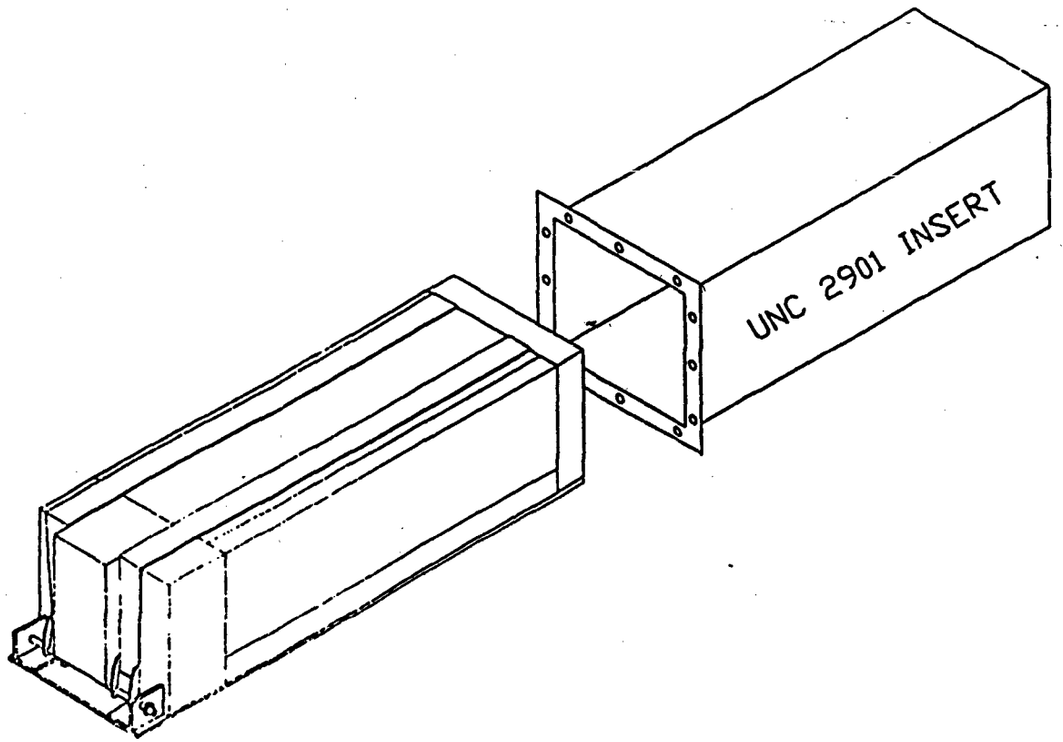

REV	BY	DATE	APP'D	DATE	DESCRIPTION

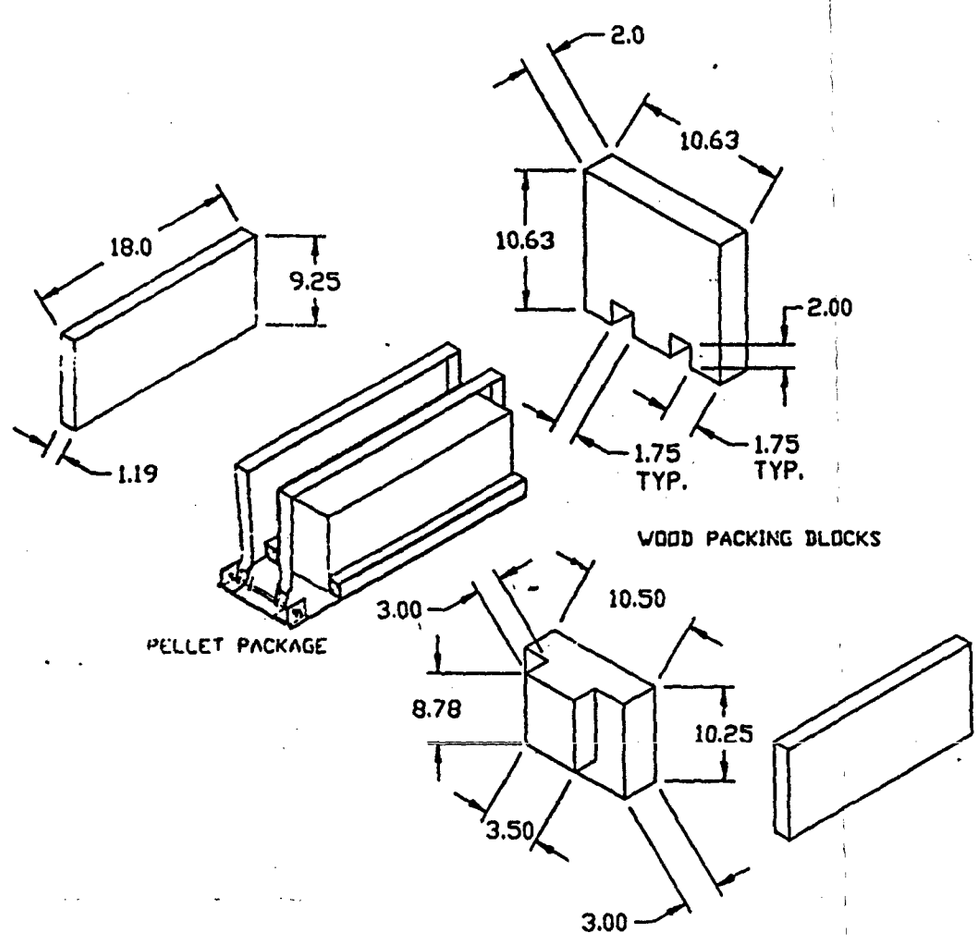

REV	BY	DATE	APP'D	DATE	DESCRIPTION

DRAWN BY: RICH JORDAN 4 / 17/95

- APPROVALS -

FACTORY MANAGER 4/18/95
FACTORY DESIGN 4/17/95
NUCLEAR POWER
REG. DRAFT 4/18/1995
OTHER/ / /9

COMBUSTION ENGINEERING

SCALE:

TOLERANCES
UNLESS OTHERWISE SPECIFIED
FRACTIONAL ±
DECIMAL ±
ANGULAR ±

WOOD SPACERS FOR
CORRUGATED TRAY SHIPMENTS

SHT 1 OF 1 DRAWING NUMBER C5018-2013 REV 0

corresponding range of water to UO_2 volume ratios is 1.78 to 0.74. Thus, the cases of interest fall below 2.5 in water to UO_2 volume ratio.

Figure 6.6 shows plots of the infinite multiplication factor versus pellet diameter for volume ratios between 0.740 and 1.784. The variation of the infinite multiplication factor is as deduced from the variation of critical mass with pellet diameter from Figure 6.3 (viz. the infinite multiplication factor is increasing with pellet diameter for these very dry mixtures of pellets and water).

6.7 UNC-2901 With Pellet Tray Package

An alternative pellet shipping configuration was designed primarily to reduce the amount of pellet dusting as a result of shipment as well as to provide the pellets in the configuration required for process conformity with the pellet to rod pushing procedure during fuel fabrication. The alternate configuration maintains the design and structure of the 2901 container from the inner compartment outward. The only modifications in design were made within the 0.0781 inch inner steel compartment.

As shown in the manufacturing drawing (D-5018-2011, Revision 0), the pellet tray package consists of layers of UO_2 pellets separated by corrugated stainless steel (SS304) trays with a final steel tray placed on top. The trays are stacked on top of the aluminum skid, and measure 1 millimeter in thickness, 45 cm in length, and 19.3 cm in width. Surrounding the trays is a 14 gauge thick stainless steel shell. The trays are completely enclosed by the shell; a seal with the base aluminum skid is formed via a silicon rubber pad and gasket. Each tray contains 12 columns of pellets stretching the entire length of the tray. The trays rest directly on the pellets and have an measured average center-to-center spacing of every other row (columns of adjacent trays are laterally offset) of 1.24 cm, based on the nominal pellet diameter of 0.819 cm, and 1.61 cm, based on the nominal pellet diameter of 0.968 cm.

It was determined that 42 layers of 0.819 cm OD pellets (with an additional tray on top - 43 total) can be stacked within the inner stainless steel shell still allowing a small void region above the top tray for the inclusion of the silicon rubber pad. Based on the larger pellet diameter of 0.968 cm, 33 layers of pellets with an additional tray and silicon pad can be loaded within the stainless steel shell.

6.7.1 Pellet Tray Model

The trays and the outer shell are illustrated in drawing D-5018-2011 Rev 0. Figure 6.10 shows the KENO model of the UNC-2901 with the tray configuration within the inner container. It should be noted that no structural material or Fiberlite is included in the region between the inner container and outer shell of the UNC-2901.

The volume of each tray was determined from the average measured weight of empty trays and the theoretical density used with the Material Input Processor (MIP LIB) used in SCALE-PC Version 4.1/0. The average measured weight per tray was 755 grams. The nominal density of SS304 is assumed to be 7.92 g/cc; therefore the average volume per tray is 95.3 cm^3. The volume within the 14 gauge stainless steel shell, which has inner dimensions of 20.24 cm x 25.84 cm x 45.32 cm, is 23,702 cm^3.

For the 0.968 cm pellet configuration, 34 trays occupy 3241.16 cm^3, the UO_2 occupies up to 13,107.35 cm^3, and the remaining volume is void. Based on the above volumes, the volume fractions of the inner container are 55.30% UO2, 13.67% SS304, and 31.03% void.

For the 0.819 cm pellet configuration, 43 trays occupy 4099.11 cm^3, the UO_2 occupies up to 11,945.12 cm^3, and the remaining volume left as void. Based on the above volumes, the volume fractions of the inner container are 50.4% UO_2, 17.29% SS304, and 32.31% void. As shown in drawing D-5018-2011, Revision 0, 2.54 cm hollow steel braces are present on each side of the steel shell. These braces were not modeled explicitly, but were replaced with wood as shown in Figure 6.10. Wooden blocks are also positioned in front of and behind the 14 gauge shell in order to increase structural stability and to reduce the amount of free volume within the inner container. The 14 gauge SS304 shell is held down by two securing straps which contour around the wooden blocks and fasten to the aluminum skid. A 7.62 cm thickness in the front of the container, which contains the straps and locking mechanisms (made up of, SS304, nylon, wood and aluminum), was not modeled; instead, in the accident case the region was conservatively left as void, and in the flooded isolated container case the region was conservatively filled with water.

Within the inner container, certain approximations are made to represent the corrugated tray and pellet configuration. The region within the 14 gauge steel shell was modeled as a homogenized region with cell weighted cross sections. The cross sections were calculated with the CSAS2X sequence in the SCALE-PC (version 4.1/0) package and the standard 27 group library. Among the options for cross section calculations, the most representative was that of the triangular pitch lattice cell.

In order to prevent over estimating the worth of the stainless steel by direct homogenization (steel, H_2O and fuel), a more conservative approach was taken. Based on a fully loaded container, the amount of steel occupied only by the trays was determined and applied as an equivalent clad thickness of 26 mils and 22 mils for the 0.819 cm diameter pellet and the 0.968 cm diameter pellet respectively. The clad thickness was kept constant around each pellet in all cases. As the number of pellets or pellet columns was reduced, the pitch was increased, and the additional steel, no longer represented as clad, was homogenized into the moderator region of the lattice cell calculation.

Since the system is so tightly packed, homogenizing the region is a valid modeling technique. However, when stacked together, the combination of the larger pellet diameter and the angle of the corrugated tray creates a direct line of sight in the horizontal direction between pellet columns. Since the effect of this gapping is not explicitly treated in the cross section development, the magnitude of this impact was investigated.

KENO Va cannot explicitly model steel trays angled at 120 degrees; therefore, a model was created based on a square pitch with 1 mm of steel representing the trays placed on two opposite corners of a bare UO_2 cylinder (Figure 6.15). This case was then compared to a cylindrical unit cell with the same amount of steel modeled explicitly as cladding, and then to an additional case which had a square cell filled with a homogenized mixture which was collapsed over the same cylindrical setup in CSAS2X (Figure 6.16). All material volumes were maintained between cases. The results shown in Figures 6.15 and 6.16 demonstrate excellent agreement between methods; each case was within one standard deviation of the others.

In order to evaluate the sensitivity due to the length of the steel modeled around each pellet, an additional set of cases were evaluated which assumed the steel on the corners covered only one half of the pellet (Figures 6.17 and 6.18). The results of these cases shown in Figures 6.17 and 6.18, as expected, showed a slightly larger deviation than the first set, on the order of 0.6%. Based on these studies, and the tightly packed configuration of the container, it is apparent that the homogenization is a reasonable technique with little uncertainty associated with it.

It was determined that the larger pellet diameter loading is a more reactive configuration at all loadings due primarily to a lower steel to UO_2 ratio. A comparison of the two pellet diameter accident scenarios is outlined in Section 6.7.3. Since it was determined that the smaller diameter pellet is less reactive, all subsequent discussion of the pellet tray configuration pertains to the larger diameter pellet size of 0.968 cm.

Administrative controls require that if less than 43 trays for the 0.819 cm pellet, or 34 trays for the 0.968 cm pellet are to be shipped per container, that the void left from the missing trays be filled with wood spacers.

6.7.2 Pellet Tray Loading Limits

The maximum loading per tray is based on the pellet diameter, the total number of rows per tray and the length of each row. The trays have 12 columns measuring 45 cm in length. The trays are not used to ship scrap pellets. The following limits have been established based on physical dimensions as well as the shipping container weight limitations.

	Small Diameter Pellet Tray Array	Large Diameter Pellet Tray Array
Number of Trays	43	34
Number of Trays Filled w/ Pellet	42	33
^{235}U Enrichment	$\leq$ 5 w/o	$\leq$ 5 w/o
Pellet Diameter (in)	0.3224 (0.819 cm)	0.3810 (0.968 cm)

6.7.3 Pellet Tray Configuration Accident Array (6x6x6)

As mentioned in Section 6.7.1, certain approximations were made to represent the corrugated tray and pellet configuration. The region within the 14 gauge stainless steel shell was modeled as a homogenized region with cell weighted cross sections. The cross sections were calculated with the CSAS2X sequence in the SCALE-PC (version 4.1/0) package using a triangular pitched lattice cell calculation and the standard 27 group library. The loading of the container was varied in order to envelope the point of maximum reactivity.

The triangular lattice cell inputs were as follows:

UO_2 Pellet O.D.	0.8189 cm	0.968 cm
Gap Thickness	0.00 cm	0.00 cm
Clad OD	0.9491 cm	1.078 cm
Pitch	Varies with Loading	Varies with Loading

As mentioned in Section 6.7.1, it was determined that if the stainless steel trays were evenly homogenized within the inner shell, the worth would be over predicted. According to the drawing, the pellets and trays are tightly packed, and the crevice of the corrugated tray actually touches a good portion of the pellet. Under flooded accident conditions, the steel which touches the pellet is less parasitic than the steel located at some distance away. For this reason, the amount of steel equal in volume to that of the tray separating each pellet was modeled as cladding material and the remaining steel content was homogenized uniformly in the moderator region of the lattice cell.

As the number of pellets or pellet columns decreases, the amount of steel representing cladding decreases, and the amount of steel in the moderator increases. This is based on the assumption that a steel tray always separates a row of pellets. Also as the number of pellets or pellet columns decrease, the equivalent unit cell pitch increases. The lattice corrected, resonance corrected, and cell weighted cross sections are then input as Nuclide 500 into the inner shell volume in KENO. This technique provides a more conservative set of cross sections than directly homogenizing the material in a mixing table.

The UO_2 loadings analyzed for the 0.968 cm diameter pellet are listed below:

Number of Pellet Columns	Pitch (cm)	Volume Fraction of SS304 in Moderator
396	1.239	0.0000
350	1.318	0.0187
300	1.424	0.0381
250	1.560	0.0566
200	1.744	0.0741
150	2.014	0.0909
100	2.466	0.1069

The accident array was run for a 6x6x6 configuration. This array was completely reflected with 12 inches of full density water. Flooding was assumed to occur in the inner container only. The exterior void regions were assumed empty to maximize container interaction. Evaluations were also preformed to determine the sensitivity of the interaction to various possible densities of the wood spacer blocks. The wide range of wood densities examined included those of Table 6-12. As expected, as the wood density increases, the interaction between the containers decreases. The results can be seen in Table 6-13 and Figure 6.11. The maximum $K_{eff} + 2\sigma$ is 0.90, which is well below the design criteria of 0.95.

The case of the smaller diameter pellet (0.819 cm) was investigated in the same manner as the larger pellet diameter accident case. As mentioned previously, this configuration is less reactive due primarily to the increased steel to UO_2 ratio. The results for two different wood densities can be seen in Table 6-14 and Figure 6.12. The maximum $K_{eff} + 2\sigma$ is 0.86, which is well below the design criteria of 0.95.

6.7.4 Pellet Tray Configuration Isolated Container

The fully flooded and reflected isolated container was analyzed. The container has the maximum loading limit of 136.5 Kgs with all void regions inside and outside of the inner compartment filled with full density water. The resulting K_{eff}'s which were calculated against various fuel loadings with the highest wood density assumed are given in Figure 6.13 and Table 6-15. In this case, as expected, the higher the wood density, the greater the reflective properties and therefore the higher system reactivity. The maximum K_{eff} $+2\sigma$ is 0.78, which is well below the design criteria of 0.95.

6.7.5 Pellet Tray Configuration Normal Transportation

The calculation supporting the normal transportation mode of operation consisted of a calculation of 512 completely dry containers stacked in an 8x8x8 array. The cross sections were calculated with CSAS2X using a uniform triangular lattice calculation. The pitch was calculated the same way as that in Section 6.7.3, with the exception of the moderator region modelled as void instead of H_2O. The containers are assumed dry and filled with 34 trays and 136.5 Kg of UO_2. The UO_2 loading is the highest achievable and therefore under dry conditions, the most reactive. This loading was run at four wood densities, although it is obvious that the highest density material is the most adverse. The results are listed in Table 6.16 and Figure 6.14. The maximum K_{eff} $+2\sigma$ is 0.61, which is well below the design criteria of 0.95.

6.7.6 Methodology Validation

The accident array configuration of UNC-2901 shipping containers is essentially a group of individually separated clusters of fuel columns sandwiched between corrugated stainless steel trays. The matter separating the fuel clusters is comprised of hydrogenous materials such as H_2O or wood blocks and layers of carbon and stainless steel. Depending on the loading assumed in each fuel cluster, the water to oxide ratio for the homogenized cluster, i.e., UO_2, H_2O, and stainless steel trays, ranges from 0.6 to 5.9. The most adverse accident conditions occur when the fuel cluster in each container is at an HO_2/UO_2 ratio of approximately 1.40, and the moderation between containers is at the lowest possible density.

In order to demonstrate how well the methodology can predict this type of system, and to assess the magnitude of any relative bias in the predicted effective multiplication factor of the SCALE-PC (version 4.1) code system, when used with the 27 group ENDF/B-IV library distributed with the code system, four classes of critical experiments were analyzed.

The first set of 13 experiments from Reference 10 consists of various 3x3 arrays of fuel rod clusters with and without steel isolation sheets at different water separation distances. These experiments provide insight into the accuracy of the methodology to calculate the interactive properties between fuel clusters when separated by full density water with and without interposed stainless steel. A summation of the results can be seen in Table 6.17, with a best estimate multiplication factor for the 13 experiments of 0.99286 ± 0.00124; the quoted uncertainty is the standard deviation about the mean of the 13 multiplication factors.

The second set involves a subset of the "Dissolution and Storage Experiments" reported by Manaranche et al in Nuclear Technology page 148, Vol. 50, 1980 (Reference 6). In these experiments, the reactivity effects of the interpositioning of hydrogenous materials of differing hydrogen densities between four water moderated PWR type assemblies are examined. These experiments should provide a measure of the ability of SCALE-PC (ver 4.1/0) to model interaction effects between heterogenous configurations of UO_2 that involve both rod cluster separation distance and hydrogenous material densities. The water to oxide ratio of the individual fuel clusters was determined to be 2.30 in all cases. Table 6-18 lists the multiplication factors for the nineteen experiments reported; the average multiplication factor for the group as a whole is 0.99911 ± 0.00695. As above, the quoted uncertainty is the standard deviation about the mean. Thus the best estimate multiplication factor for the group exhibits a negligible bias relative to unity.

The above two sets of experiments employed aluminum clad UO_2. The case of the UO_2 pellets aligned in 1 mm thick stainless steel corrugated trays is analogous to an array of stainless steel clad UO_2 pellet columns. The third set of experiments employs 16 mil stainless steel clad instead of the nearly transparent aluminum employed in the first two sets of experiments. The six fully reflected "uniform" rod lattice configurations of 2.70 w/o enriched UO_2 reported in YAEC-94 (Reference 11) and WCAP-1412 (Reference 12) are used here. These experiments contain rods with stainless steel clad UO_2 wherein the clad material composition is based on the quoted chemical analysis. The experiments range over water to oxide ratios of 1.0 to 5.0. The analysis of these experiments demonstrates the ability of the SCALE-PC (version 4.1/0) model to calculate the worth of relatively thick stainless steel 304 clad material in UO_2 lattices. In these lattices, approximately 8 to 10% of the fractional absorptions are within SS304. The resulting average k-effective and standard deviation about the mean for the 6 experiments are 0.99193 and ± 0.0023; the individual values are listed in Table 6.19.

UNC-2901 Shipping Container

The final set of experiments are CE proprietary critical experiments (Reference 13) which were carried out at the Westinghouse CRX facility with 2.719 w/o enriched UO_2 clad in aluminum. The 29 lattices analyzed consist of 10 with a basic unit cell pitch of 0.575 inches and 19 at 0.600 inches. The water to oxide ratios were 1.260 and 1.494 respectively, for the unit fuel rod cells. The configurations examined consisted of uniform square and rectangular arrays of fuel pins with and without internal (1x1 and 2x2) water holes. Thus, these lattices mock up a range of effective H/U ratios characteristic to the postulated rectangular pellet column arrays in the shipping containers with varying numbers of missing internal pellet columns. These effective H/U ratios (3.7 to 5.0) span the more reactive shipping container loadings shown in Figure 6.11. The results of these 29 cases are listed in Table 6.20 and have an average K-effective of 0.98686 with a standard deviation about the mean of $\pm$ 0.00325.

The data in Figure 6.11 indicates that the most reactive condition for the corrugated tray configuration occurs at a water to oxide ratio of approximately 1.4. The implied bias in the more limiting postulated accidents, based on the analyses of the above sets of experiments, is small relative to the 5% margin to 0.95.

6.8 References

1. L. M. Petrie and N. F. Cross, "KENO-IV, An Improved MONTE CARLO Criticality Program," ORNL-2938, November, 1975.

2. "SCALE: A Modular Code System for Performing Standardized Computer Analysis for Licensing Evaluation - Book II", NUREG/CR-0200.

3. G. R. Handley and C. M. Hopper, "Validation of the "KENO" Code for Nuclear Criticality Safety Calculations of Moderated, Low-Enriched Uranium Systems", Y-1948, June 13, 1974.

4. N. M. Green, et al, "AMPX: A Modular Code System for Generating Coupled Neutron-Gamma Libraries from ENDF/B", ORNL/TM-3706, March 1976.

5. W. R. Cable, "123 Group Neutron Cross Section Data Generated from ENDF/B-II Data for use in the XSDRN Discrete Ordinates Spaectral Averaging Code", DLC-16, Radiation Shielding Information Center, 1971.

6. J. C. Manaranche, et al, "Dissolution and Storage Experiment with 4.75 w/o U-235 Enriched UO2 Rods", Nuclear Technology, Vol 50, pg 148, September 1980.

7. "Critical Experiments Supporting Underwater Storage of Tightly Packed Configurations of Spent Fuel Pins", - Summary Report, M. N. Baldwin, G. S. Hoovler, E. L. Maceda, F. G. Welfare; Babcock & Wilcox Co., BAW-1645-4, November 1981.

8. H. K. Clark, "Critical and Safe Masses and Dimensions of Lattices of U and UO2 Rods in Water", DP-1014 Savannah River Laboratory, February 1966.

9. SCALE-PC, Standardized Criticality Analyses and Licensing Evaluation code, (version 4.1/0), 9/29/93.

10. "Critical Experiments Supporting Close Proximity Water Storage of Power Reactor Fuel", - Summary Report, M. N. Baldwin, G. S. Hoovler, R. L. Eng, F. G. Welfare; Babcock & Wilcox Co., BAW-1484-7, July, 1979.

11. "Yankee Critical Experiments- Measurement on Lattices of Stainless Steel Clad Slightly Enriched Uranium Dioxide Rods in Light Water"; P. W. Davison, et al; APD, West. El. Corp., YAEC-94, April 1, 1959.

12. "Results of Critical Experiments in Loose Lattices of UO2 Rods in H2O"; V. E. Grob, P. W. Davison, D. F. Hanlen, R. D. Leamer, F. L. Kelley, J. D. Cleary; Westinghouse Electric Corp.; WCAP-1412, March 30, 1960.

13. A. Vukmir, et al, "Critical Experiments for Combustion Engineering, Inc.", WCAP-7102, April 1968, - Westinghouse Confidential.

UNC-2901 Shipping Container

Figure 6.10
KENO Va Model Of UNC-2901

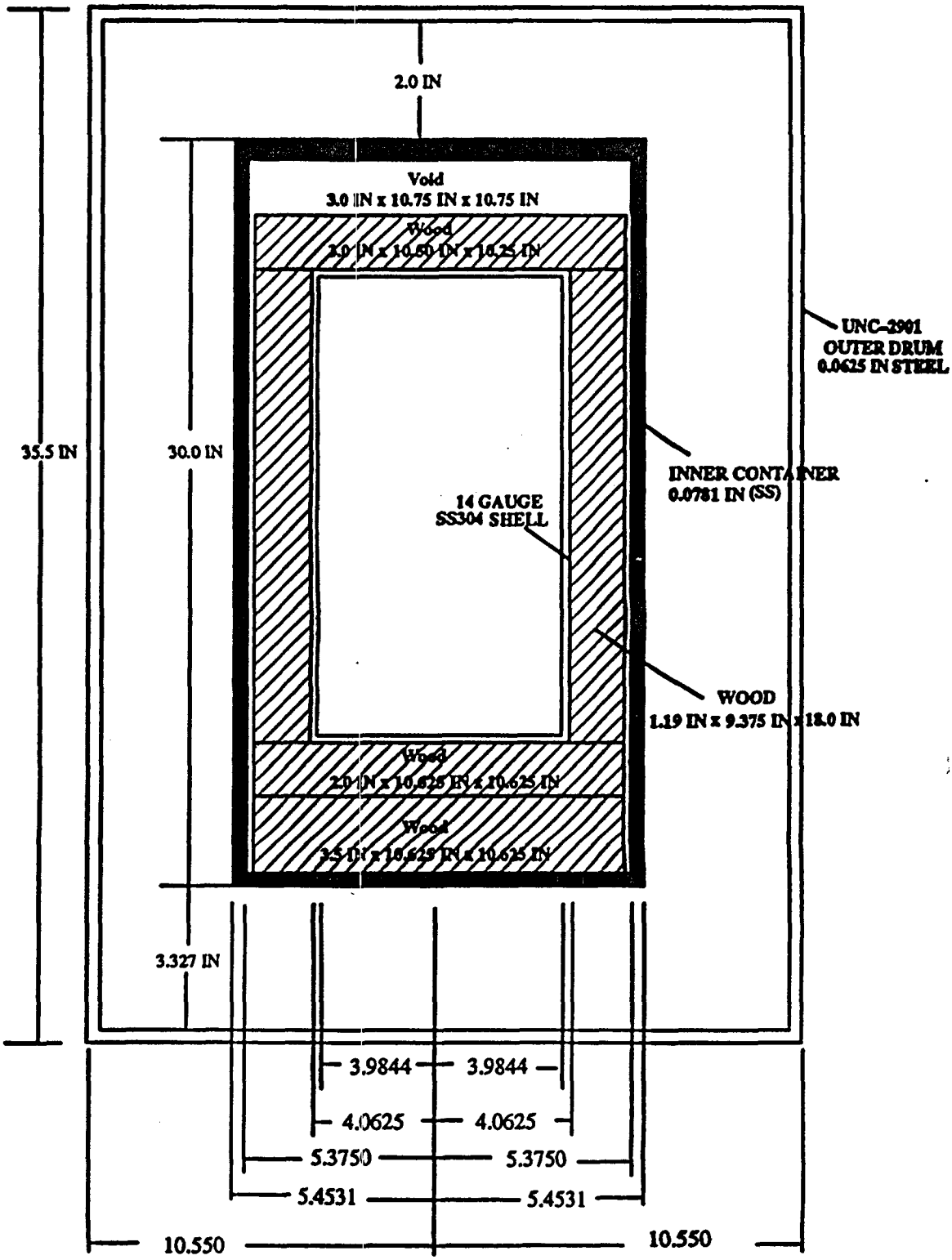

Figure 6.11
K_{eff} + 2σ versus $KgUO_2$
Pellet Tray Configuration, 6x6x6 Accident Array
Large Diameter (0.968 cm) Pellet

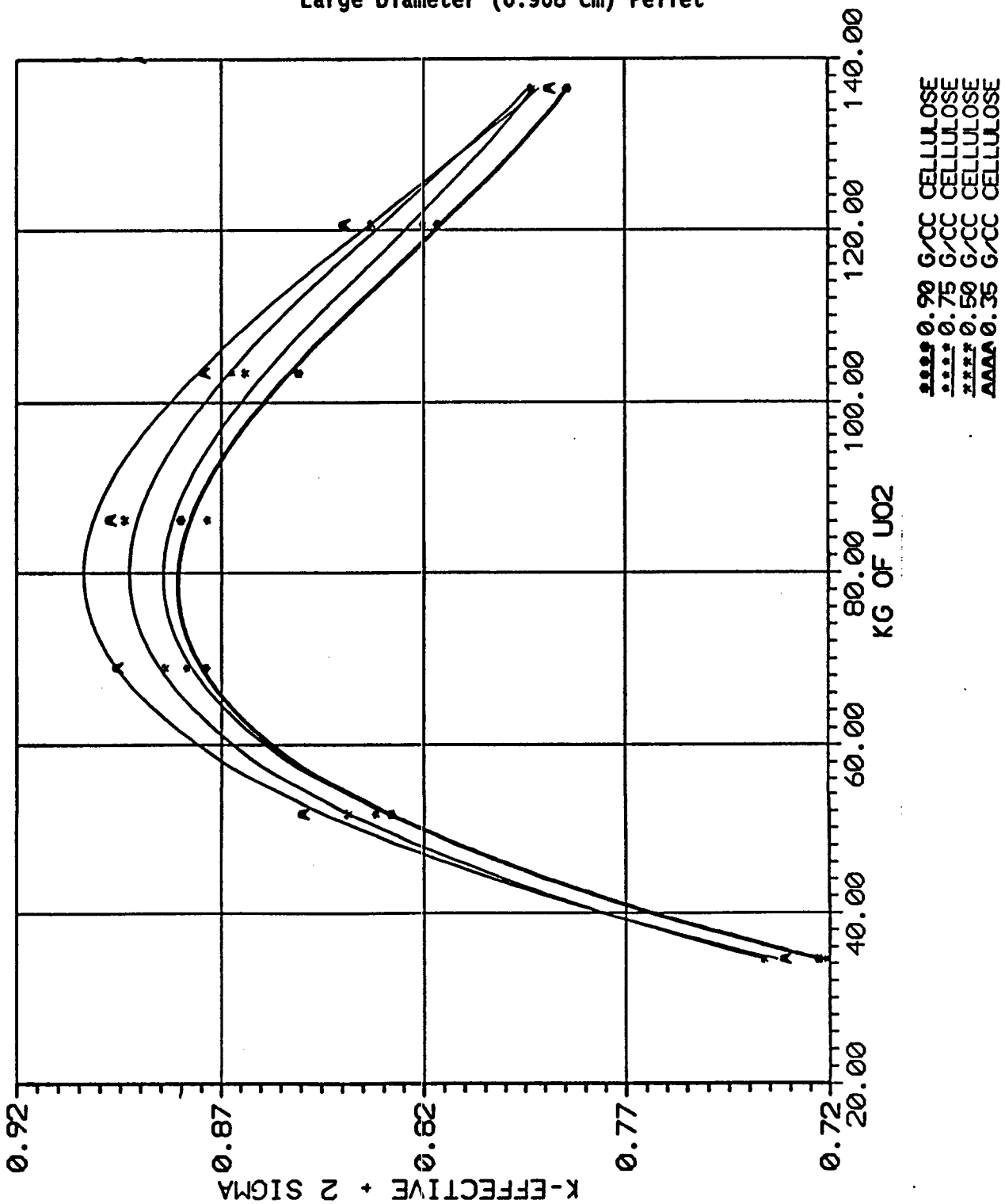

Figure 6.12
K_{eff} + 2σ versus $KgUO_2$
Pellet Tray Configuration, 6x6x6 Accident Array
Small Diameter (0.819 cm) Pellet

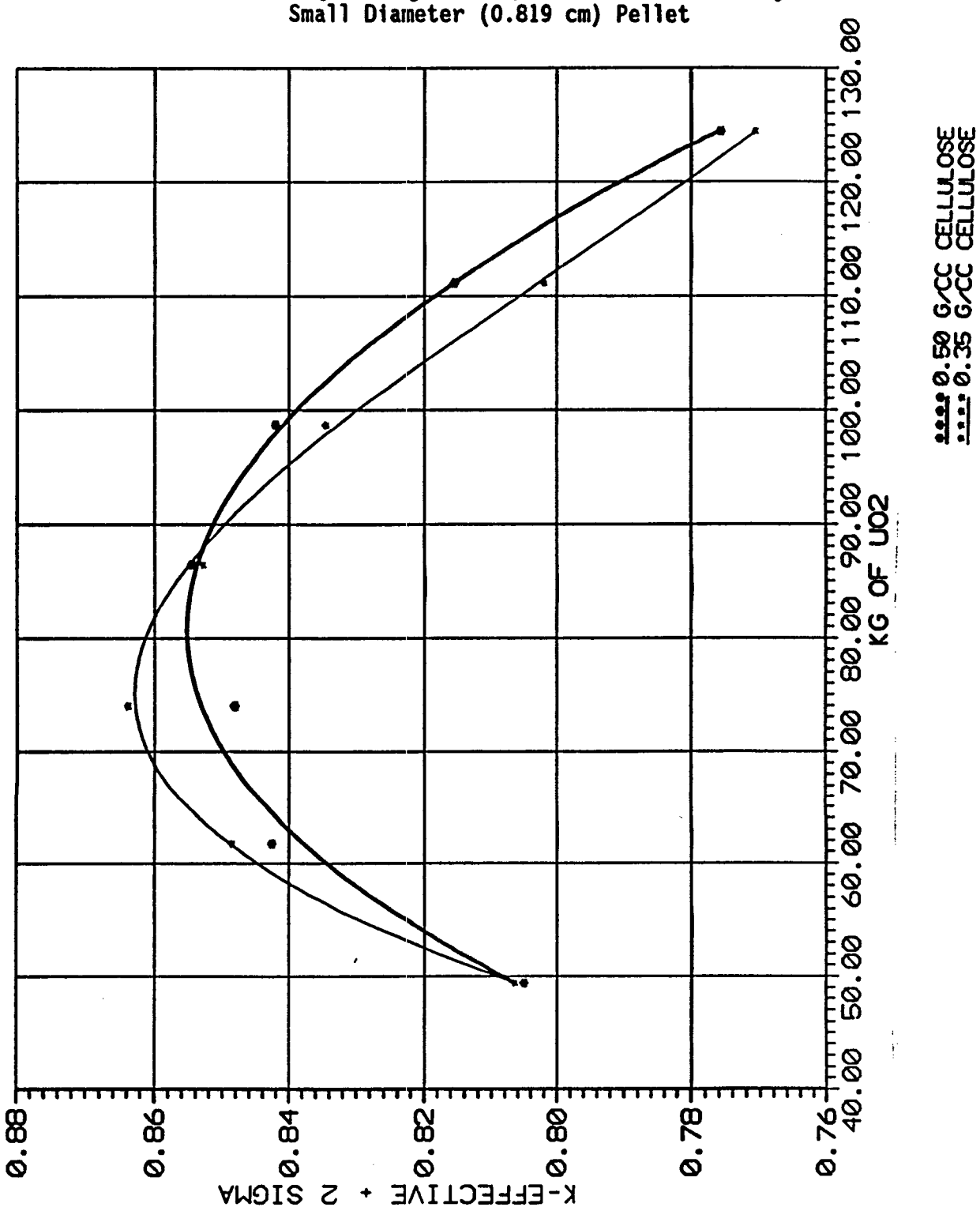

Figure 6.13
K_{eff} + 2σ versus $KgUO_2$
Pellet Tray Configuration, Isolated Container

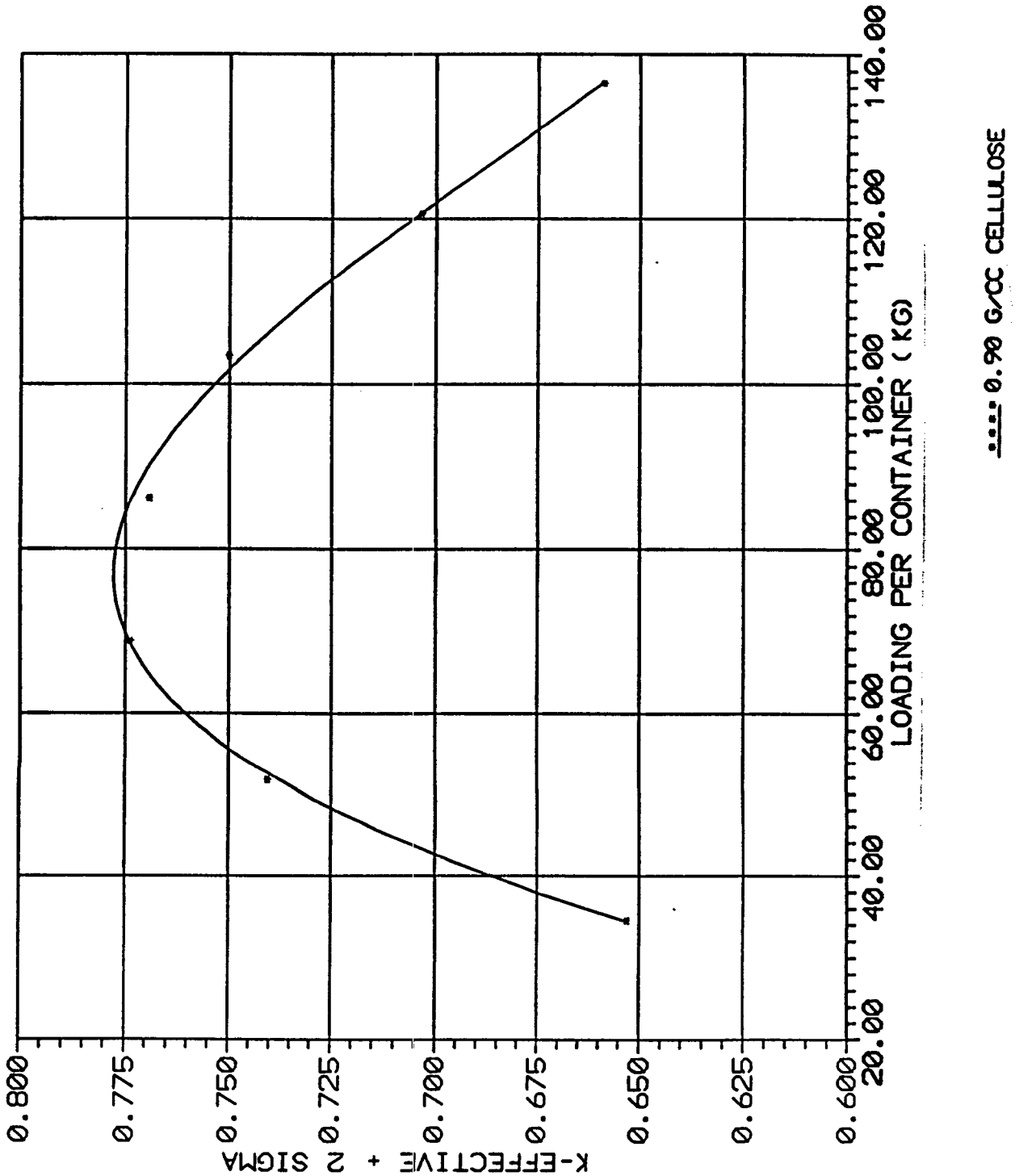

Figure 6.14
K_{eff} + 2σ versus Wood Density
Pellet Tray Configuration, 8x8x8 Normal Transportation Mode
136.5 Kg Loading

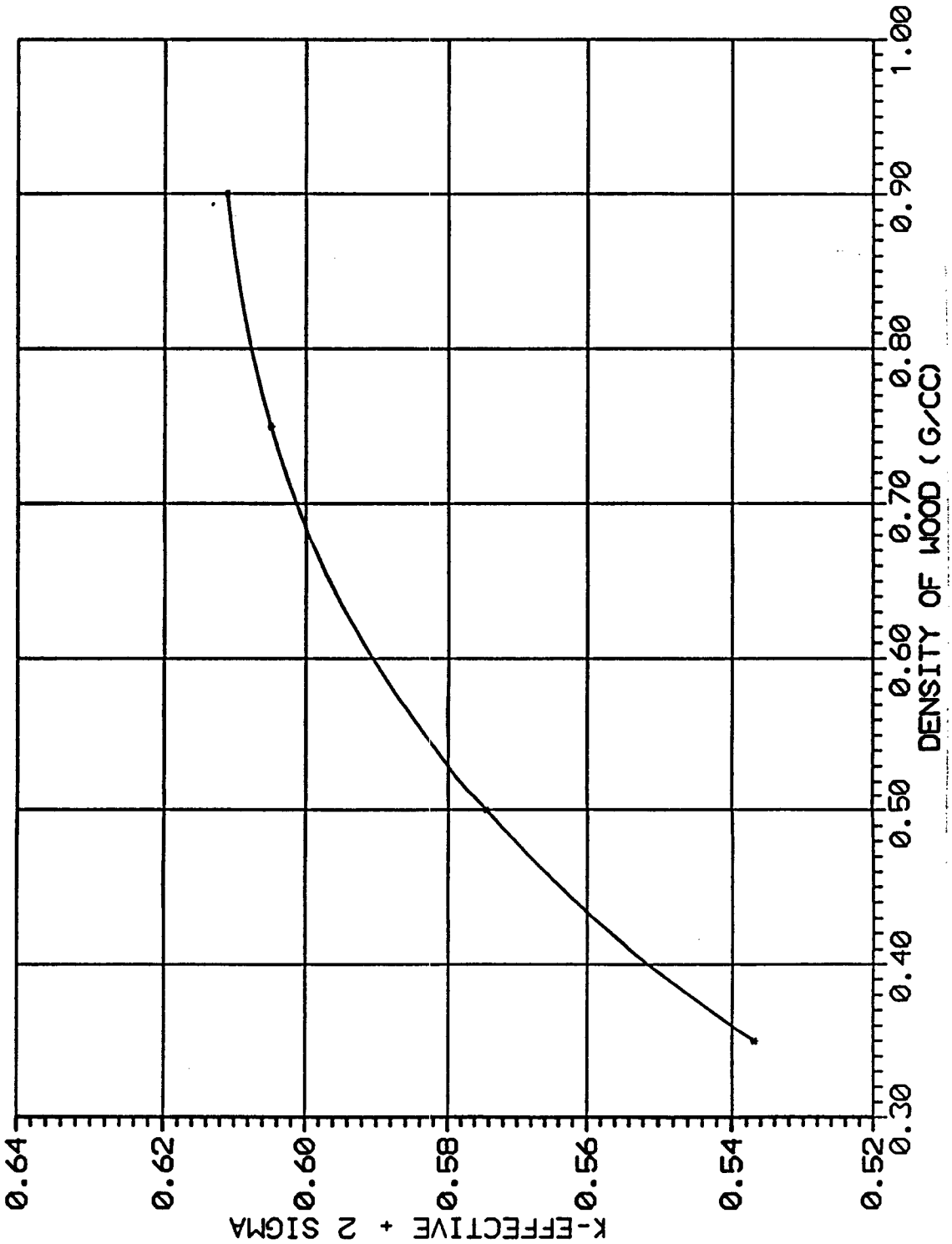

Figure 6.15
KENO Va Model of Steel Trays (3/4 length)

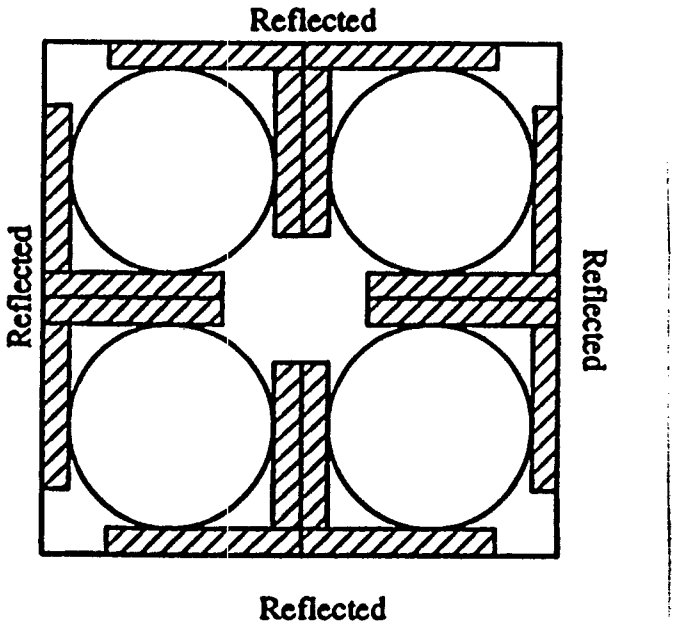

(K-effective = 1.08402 + 0.00247)

Figure 6.16
KENO Va Model Approximating 3/4 Length Steel Model

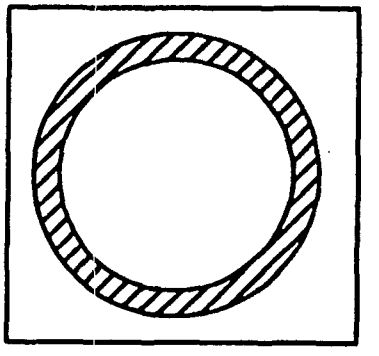

(K–effective = 1.08376 + 0.00247)

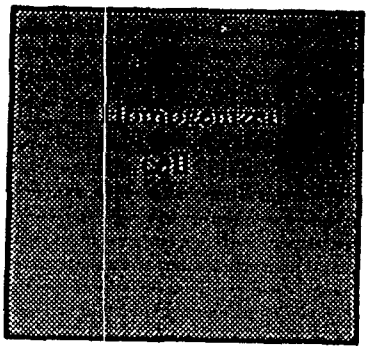

(K–effective = 1.08197 + 0.00242)

Figure 6.17
KENO Va Model of Steel Trays (1/2 length)

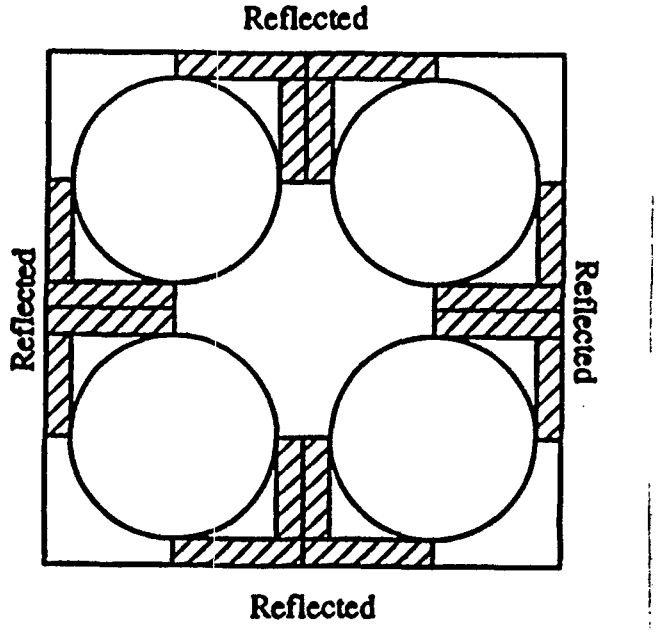

(K-effective = 1.14811 + 0.00241)

Figure 6.18
KENO Va Model Approximating 1/2 Length Steel Model

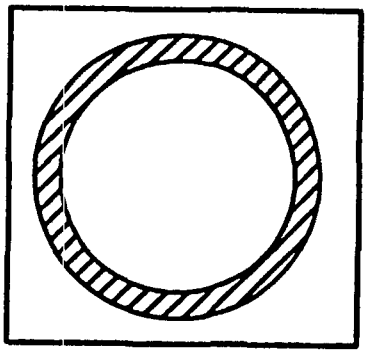

(K-effective = 1.14776 + 0.00268)

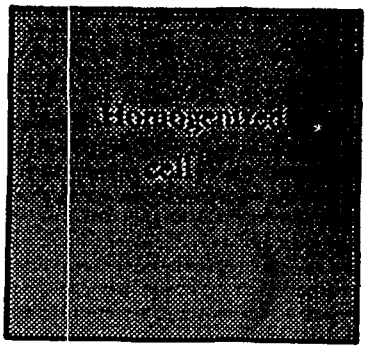

(K-effective = 1.14189 + 0.00246)

Table 6-12
Densities of Various Wood Types

Wood Type	Grams/cc
Ash	0.65 - 0.85
Birch	0.51 - 0.77
Cedar	0.49 - 0.57
Dogwood	0.76
Elm	0.54 - 0.60
Maple	0.62 - 0.75
Oak	0.60 - 0.90
Pine	0.35 - 0.60
Poplar	0.35 - 0.50

Table 6-13
Pellet Tray Configuration 6x6x6 Accident
Case Results for Various Wood Densities
Large Diameter (0.968 cm) Pellet

Total Kgs	0.90 g/cc Cellulose	0.75 g/cc Cellulose	0.50 G/cc Cellulose	0.35 g/cc Cellulose
136.5	0.77715 ± 0.00355	0.78670 ± 0.00321	0.78656 ± 0.00338	0.78121 ± 0.00375
120.6	0.80861 ± 0.00386	0.81263 ± 0.00377	0.82524 ± 0.00384	0.83208 ± 0.00360
103.4	0.84324 ± 0.00368	0.85996 ± 0.00371	0.85630 ± 0.00303	0.86740 ± 0.00343
86.2	0.87250 ± 0.00381	0.86662 ± 0.00346	0.88594 ± 0.00396	0.88954 ± 0.00387
68.9	0.86684 ± 0.00360	0.87115 ± 0.00379	0.87565 ± 0.00420	0.88841 ± 0.00357
51.7	0.82137 ± 0.00241	0.82468 ± 0.00365	0.83155 ± 0.00358	0.84208 ± 0.00362
34.5	0.71650 ± 0.00318	0.71468 ± 0.00320	0.73005 ± 0.00316	0.72535 ± 0.00288

Table 6-14
Pellet Tray Configuration, 6X6X6 Accident Array
Small Diameter (0.819 cm) Pellet

Total Kilograms	0.50 g/cc Cellulose	0.35 g/cc Cellulose
124.4	0.76868 ± 0.00349	0.76464 ± 0.00302
111.1	0.80786 ± 0.00381	0.79533 ± 0.00333
98.7	0.83525 ± 0.00337	0.82732 ± 0.00361
86.4	0.84761 ± 0.00346	0.84624 ± 0.00337
74.0	0.84151 ± 0.00333	0.85727 ± 0.00329
61.7	0.83547 ± 0.00356	0.84180 ± 0.00341
49.4	0.79829 ± 0.00338	0.79983 ± 0.00334

Table 6-15
Pellet Tray Configuration, Isolated Container

Total Kilograms	0.90 g/cc Cellulose
135.6	0.65159 ± 0.00360
120.6	0.69564 ± 0.00392
103.4	0.74245 ± 0.00381
86.2	0.76077 ± 0.00420
68.9	0.76601 ± 0.00391
51.7	0.73306 ± 0.00376
34.5	0.64648 ± 0.00324

Table 6-16
Pellet Tray Configuartion, 8X8X8 Normal Transportation Mode

Density of Cellulose	$K_{eff} \pm \sigma$
0.90	0.60688 ± 0.00213
0.75	0.60087 ± 0.00207
0.50	0.57042 ± 0.00201
0.35	0.53298 ± 0.00200

Table 6-17
B&W Critical Experiments
Supporting Close Proximity Water Storage of
Power Reactor Fuel

B&W Experiments, 1484-7	
Experiment #	$K_{eff} \pm \sigma$
Core I	0.99295 ± 0.00302
Core II	0.99389 ± 0.00266
Core III	0.99312 ± 0.00255
Core IX	0.99111 ± 0.00282
Core X	0.99261 ± 0.00303
Core XIa	0.99103 ± 0.00263
Core XIb	0.99315 ± 0.00276
Core XIc	0.99332 ± 0.00293
Core XId	0.99410 ± 0.00272
Core XIe	0.99551 ± 0.00265
Core XIf	0.99226 ± 0.00231
Core XIg	0.99163 ± 0.00270
Core XII	0.99254 ± 0.00270

Table 6-18
Dissolution and Storage Experiments

Asembly Configuration					Calculated $K_{eff} \pm \sigma$
Δ cm	Interstitial Material	Compounds		Critical Water Height cm	Moderator in Cruciform at Critical Water Height
		Density g/cc	Conc H g/cc		
0	Water	1.0	0.1119	23.80	1.00316 ± 0.00377
2.5	Box + Air	0	0	29.03	0.99148 ± 0.00385
	Box + $(C_8H_8)_n$	0.0323	0.0025	28.61	0.98975 ± 0.00362
	Box + Powder $(CH_2)_n$	0.2879	0.0414	26.98	1.00042 ± 0.00346
	Box + Balls $(CH_2)_n$	0.5540	0.0800	25.54	0.99644 ± 0.00346
	Box + Water	1.0	0.1119	25.66	1.00621 ± 0.00327
	Water	1.0	0.1119	24.48	0.99570 ± 0.00338
5.0	Box + Air	0	0	34.48	0.99401 ± 0.00344
	Box + $(C_8H_8)_n$	0.0262	0.0020	34.39	0.98770 ± 0.00344
	Box + Powder $(CH_2)_n$	0.3335	0.0480	30.16	1.00236 ± 0.00378
	Box + Balls $(CH_2)_n$	0.5796	0.0833	30.73	1.00650 ± 0.00346
	Box + Water	1.0	0.1119	32.78	1.01158 ± 0.00368
	Water	1.0	0.1119	31.47	0.99499 ± 0.00341
10.0	Box + Air	0	0	46.08	1.00385 ± 0.00391
	Box + $(C_8H_8)_n$	0.0288	0.0022	45.62	0.99517 ± 0.00392
	Box + Powder $(CH_2)_n$	0.3216	0.0464	42.05	1.00820 ± 0.00370
	Box + Balls $(CH_2)_n$	0.5680	0.0816	49.94	1.00669 ± 0.00375
	Box + Water	1.0	0.1119	64.12	0.99749 ± 0.00338
	Water	1.0	0.1119	64.34	0.99130 ± 0.00356

Table 6-19
WAPD/CRX Yankee Experiments

WAPD/CRX Yankee Experiments		
Experiment #	H_2O/UO_2	$K_{eff} \pm \sigma$
1	1.048	0.98990 ± 0.00270
2	1.405	0.99390 ± 0.00280
3	1.853	0.98830 ± 0.00290
4	3.373	0.99340 ± 0.00270
5	4.078	0.99370 ± 0.00320
6	4.984	0.99240 ± 0.00290

Table 6-20
Critical Experiments for Combustion Engineering

CE Experiments, WCAP-7102	
Experiment #	$K_{eff} \pm \sigma$
Core 01	0.99304 ± 0.00312
Core 03	0.98142 ± 0.00301
Core 05	0.98491 ± 0.00293
Core 06	0.98315 ± 0.00300
Core 07	0.99048 ± 0.00290
Core 08	0.98593 ± 0.00278
Core 09	0.98683 ± 0.00277
Core 10	0.98911 ± 0.00281
Core 14	0.97957 ± 0.00282
Core 15	0.98557 ± 0.00273
Core 18	0.98634 ± 0.00264
Core 22	0.99030 ± 0.00287
Core 26	0.99022 ± 0.00266
Core 31	0.98706 ± 0.00292

CE Experiments, WCAP-7102	
Experiment #	$K_{eff} \pm \sigma$
Core 38	0.98607 ± 0.00316
Core 39	0.98752 ± 0.00242
Core 41	0.99086 ± 0.00303
Core 42	0.98277 ± 0.00293
Core 46	0.99077 ± 0.00283
Core 86	0.98887 ± 0.00278
Core 87	0.98349 ± 0.00296
Core 88	0.98641 ± 0.00293
Core 89	0.98672 ± 0.00304
Core 90	0.99163 ± 0.00293
Core 91	0.98610 ± 0.00282
Core 94	0.98295 ± 0.00290
Core 106	0.98662 ± 0.00296
Core 107	0.98496 ± 0.00266
Core 110	0.98928 ± 0.00288